

# Maximizing Nitrate Absorption of Agricultural Waste Water in a Tubular Microalgae Reactor by Adapting the Illumination Spectrum

J. Martin, A. Dannenberg, G. Detrell, R. Ewald, S. Fasoulas

**Abstract**—Microalgae-based photobioreactors (PBR) for Life Support Systems (LSS) are currently being investigated for future space missions such as a crewed base on planets or moons. Biological components may help reducing resupply masses by closing material mass flows with the help of regenerative components. Via photosynthesis, the microalgae use CO<sub>2</sub>, water, light and nutrients to provide oxygen and biomass for the astronauts. These capabilities could have synergies with Earth applications that tackle current problems and the developed technologies can be transferred. For example, a current worldwide discussed issue is the increased nitrate and phosphate pollution of ground water from agricultural waste waters. To investigate the potential use of a biological system based on the ability of the microalgae to extract and use nitrate and phosphate for the treatment of polluted ground water from agricultural applications, a scalable test stand is being developed. This test stand investigates the maximization of intake rates of nitrate and quantifies the produced biomass and oxygen. To minimize the required energy, for the uptake of nitrate from artificial waste water (AWW) the Flashing Light Effect (FLE) and the adaption of the illumination spectrum were realized. This paper describes the composition of the AWW, the development of the illumination unit and the possibility of non-invasive process optimization and control via the adaption of the illumination spectrum and illumination cycles. The findings were a doubling of the energy related growth rate by adapting the illumination setting.

**Keywords**—Microalgae, illumination, nitrate uptake, flashing light effect.

## NOMENCLATURE

### A. Acronyms

IRS	Institute of Space Systems
LED	Light Emitting Diode
FPA	Flat Panel Airlift
SGW	Synthetic Ground Water
GW	Ground Water

## II. BACKGROUND

AFTER several years of research and development for microalgae in space applications, such as hybrid LSS, the IRS also focusses on transferring the learned knowledge of process control to terrestrial applications. One of the possible applications is the field of water treatment of agricultural waste waters. Overfertilisation can be attributed to the leaching of fertilizers in agriculture and is associated with high

levels of nitrate and phosphate in groundwater (GW) [1]. This results in the eutrophication of affected waters and is a problem with far reaching effects worldwide [2]. Filtration processes lead to highly concentrated remnant and shift the problem [3]. Biological processes offer an alternative [4], in particular the use of microalgae for the absorption of Nitrate and Phosphate offers the possibility to add a value creation to the chain of waste water treatment by using the biomass and the local CO<sub>2</sub> sink.

The overriding goal of the presented research project is an optimized and automated reduction of nitrate and phosphate in GW using microalgae as biological component.

## III. SCALABLE REACTOR SYSTEM AND IL TEST STAND

### A. Requirements and Parameters of Optimization

The developed reactor system shall use the nitrate and phosphate from polluted ground water to cultivate microalgae and provide a value adding link to the chain of water treatment. Fig. 1 shows the general mass flows of the system. To further identify subsystems and components, objectives and requirements are determined. The main objective is to maximize the capability of nitrate uptake and the biomass productivity in relation to the required energy and maintenance efforts.

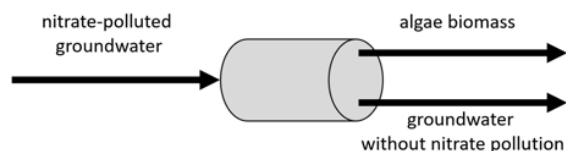


Fig. 1 Inputs and Outputs of the PBR-System

Another objective is the scalability of the system and transferability of cultivation optimizations from a small scale teststand to a larger system.

The requirements on the system are:

- Reduction of NO<sub>3</sub> and PO<sub>4</sub> below legal limits
- Operability with different types of GW
- No contamination of GW with microalgae

### B. System Concepts

In order to achieve the requirements, different approaches are possible. Figs. 2 and 3 present different options. Either the nitrate and phosphate are extracted from the GW in a separated filtration unit, or the PBR is fed directly with GW.

J. Martin is with the Institute of Space Systems, University of Stuttgart, Germany (corresponding author, phone: +49-711-685-62391; e-mail: martin@irs.uni-stuttgart.de).

Prefiltration comes with the advantage that the cultivation is separated from the GW. That eliminates the risk of contaminating the treated GW with microalgae and allows to control and maintain the cultivation conditions in the PBR for changing concentrations in the GW. Fluctuations in the quantities of substances in the GW will not influence the cultivation. A physico-chemical prefiltration will also increase the buffer capabilities and the modular expandability. For this project, the concept of prefiltration was chosen for further analysis due to decisive advantages:

- Separation of cultivation from GW
- ➔ no risk of GW contamination
- Higher concentrations in the reactor
- ➔ smaller reactors possible
- Dosage of nutrients in the reactor
- ➔ reproducible process control
- Fluctuations in the quantities of substances in the GW have no influence on cultivation
- Higher product quality through controllable cultivation parameters
- Same applicability for different GW types
- Modular expandability/connectivity of the system to other applications

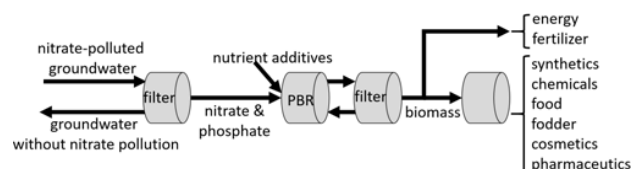


Fig. 2 Concept of prefiltration

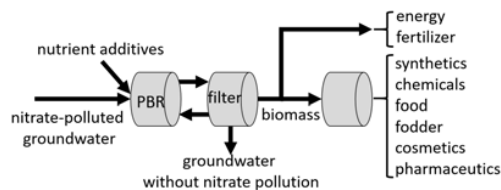


Fig.3 Concept of direct input

### C. Reactor Geometry and Scalability

The reactor geometry provides the environment for the microalgae to meet the defined requirements. The geometry of the PBR has an influence on mixing behavior, flow dynamics and light distribution [5]. Another impact of the geometry is on the biofilm formation, the required cleaning effort and manufacturing costs.

To increase the energy efficiency of the microalgae cultivation, the FLE can be used [6]. The FLE describes the effect that the biochemical process of photosynthesis in a cell requires only about 10% of the time light energy input [7], [8]. This effect can be used to maximize the growth rate per light energy either with constant illumination by a strong illumination intensity gradient and geometry induced vortices or by a homogeneous light distribution with a blinking illumination unit. Fig. 4 shows the comparison of the simulated light field of different reactor geometries. For all

compared geometries, an air lift driven mixing is assumed. A tubular reactor in blue, in which the air flows from the bottom to the top of a transparent tube and the light hits the surface perpendicular in each point is compared to a FPA reactor. For the tubular reactor, the FLE would be realized by a blinking of the light unit, so a constant light distribution is desired. The FPA could use either a blinking light unit from both sides (orange), where also a constant distribution of the light is desired, or a constant illumination from one side and high intensity gradient combined with geometry induced barrel role swirls in the flow (yellow) [8]. For this simulation approach, an illumination flux  $I_0$  of  $400 \mu\text{mol/s}\cdot\text{m}^2$  was assumed as this intensity delivered good growth rates without photoinhibition. An illumination of 680 nm wavelength and a biomass  $DS$  of  $0.2312 \text{ kg/m}^3$  *Chlorella vulgaris* were chosen due to good experimental experience with these settings. This was the chosen setup, due to the availability of data on algae and wavelength specific absorption coefficients  $\epsilon_s$  and due to previously obtained experience with light intensities [9]-[13]. The simulation has been done with Matlab R2018b and is based on the absorption principal of the Lambert Beer Law, as shown in (1) [14], [15]. Here, the simulation is summarized; it has been previously presented in [13].

$$\log_{10}\left(\frac{I_0}{I}\right) = \epsilon_s \cdot DS \cdot L \quad (1)$$

The simulation calculates the resulting light flux intensity for every level of depth by integrating all incoming rays analytically. Due to the assumption that all rays are perpendicular to the surface, a focal point occurs for the tubular reactor at the center. The focusing of light towards the center of the tubular reactor leads the compensation of the absorbed intensity and creates a homogeneous light field.

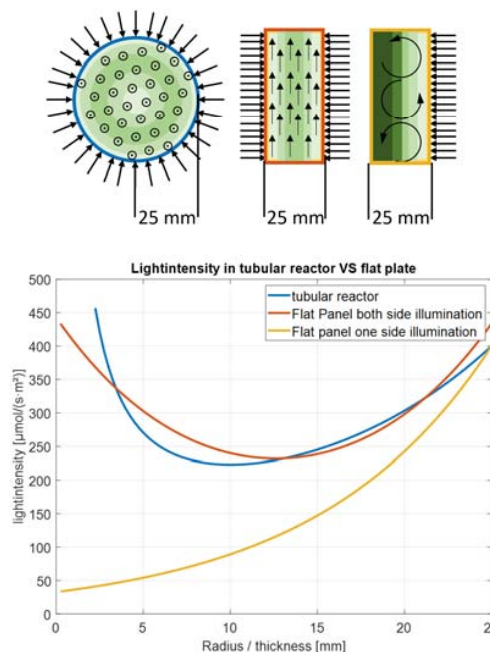


Fig. 4 Simulation of light intensity through different reactor types

The both sided illuminated FPA (red) has a similar light distribution than the tubular reactor. If the realization of the FLE could be made possible by the illumination unit, these concepts would be more suitable for the desired application due to the simplicity of the geometries. Static mixers complicate the production and the cleaning processes. To evaluate the viability of the red and blue options, a study was carried out to determine whether the FLEs can be induced and save energy by using LEDs and what other advantages are associated with controllable lighting (as described in Section III).

The tubular reactor was preferred for this application since the cleaning of a tube can be done mechanically while in an FPA, mechanical cleaning is difficult. The surface to volume ratio is smaller, for a tubular reactor compared to a FPA with  $r = d$ , as shown in Fig. 5 and Table I so less problems with biofilm building can be expected.

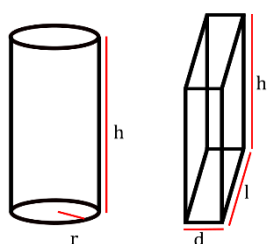


Fig.5 nomenclature for calculation

TABLE I SURFACE TO VOLUME RATIO		
	Tubular Reactor	Flat Panel Reactor
Volume	$\pi \cdot r^2 \cdot h$	$h \cdot l \cdot d$
Surface	$2 \cdot \pi \cdot r \cdot h$	$2 \cdot h \cdot l + 2 \cdot h \cdot d$
Surface/Volume	$\frac{2}{r}$	$\frac{2}{d} \cdot \left(\frac{l+d}{l}\right)$

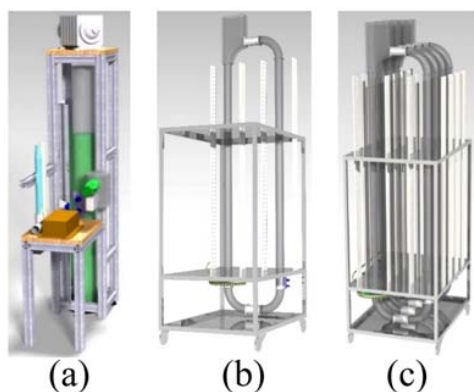


Fig. 6 Test stands with reactor capacities: (a) 1 liter, (b) 6 liters, (c) 24 liters

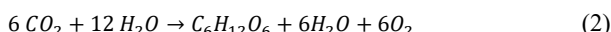
For this project, round profiles with a diameter of 50 mm were selected as the reactor geometry.

First, a 1-liter test stand is built to demonstrate the functionality of the reactor system setup in combination with the illumination unit, to develop the sensor unit and to carry

out optimizations. A 6-liter reactor will then be set up to demonstrate the transferability of measurements from the small system to a larger one. Afterwards the 6-liter system can be scaled in parallel. Scaling to 24 liters is planned. Fig. 6 shows the steps of the planned test stands.

#### IV. ILLUMINATION UNIT

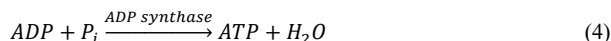
The illumination unit supplies the algae with sufficient light for photosynthesis to take place. The physiological process of photosynthesis is an essential cornerstone that enables the algae to be used for the stated purposes. In oxygen photosynthesis,  $\text{CO}_2$ ,  $\text{H}_2\text{O}$  and light radiation are transformed into glucose ( $\text{C}_6\text{H}_{12}\text{O}_6$ ) and  $\text{O}_2$ :



In detail the process consists of two parts: the light reaction and the dark reaction. In the light reaction the energy of the collected photons is converted into chemical energy. For this purpose, the water is split in the photolysis (3), oxygen escapes to the environment and hydrogen is chemically bound. The described complex is located in the thylakoid membrane, in which the photo systems are embedded [16].



Through the electron transport chain the electrons then move from the inside of the thylakoid membrane to the outside (the light side) or protons from the outside to the inside. The resulting electrochemical potential is converted into chemical energy in the adeno-sintriphosphate synthase. In this process, adenosine diphosphate (ADP) is converted with phosphate ( $\text{P}_i$ ) into water and adenosine triphosphate (ATP) () [16], [17].



Subsequently, the NADPH and ATP molecules are further processed in the dark reaction. In this cycle (the Calvin cycle) [7], the energy stored in the ATP molecules is used to perform the reaction (2) and  $\text{CO}_2$  is incorporated into glucose or oxygen is released. During this dark phase, no light energy is required. Providing light with the illumination unit, in a frequency where it can be used by the photosystem, thus increasing the energetic efficiency was the goal for the development of the illumination unit.

Required light intensity levels at the surface of the tubular reactor are between  $40 \mu\text{mol/s m}^2$  and  $1000 \mu\text{mol/s m}^2$ , depending on the biomass concentration [18], [19]. Due to the round reactor geometry, the light must be pulsable to produce the FLE. To achieve a high photon efficiency, LEDs were chosen. Another optimization strategy is to cover the relevant absorption spectrum by the selection and control of individual LEDs. An adaptable illumination spectrum could also give the option of non-invasive process control [20], [21]. Fig. 7 shows the absorption spectrum of *C.vulgaris* and different pigments

found in the microalgae [22], [23]. Chlorophyll a & b are photoactive pigments, and the illumination unit should match their absorption spectrum to reach a higher degree of efficiency. Fig. 8 shows the result of a simulation trying to optimize the matched spectrum with eight different LEDs by picking eight different LED-spectra from a database and adjusting the intensities individually.

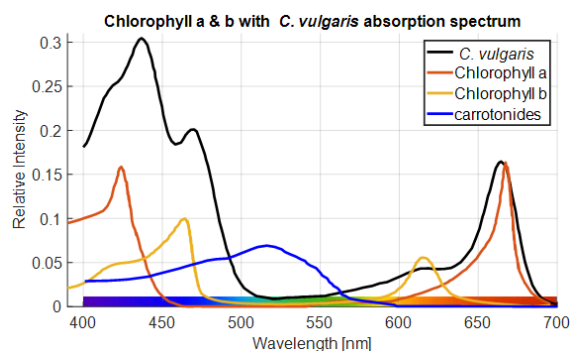


Fig. 7 Absorption spectra of *C. vulgaris* and different pigments

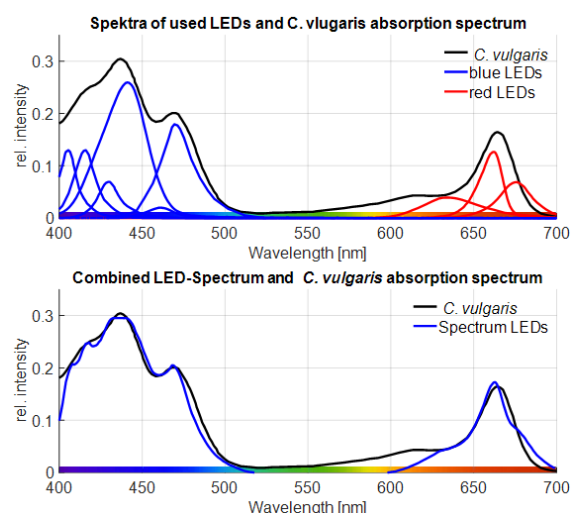


Fig. 8 Spectrum matching simulations

Fig. 9 shows the developed light unit from the circuit diagram to the first prototype. The shown light unit has eight types of LEDs with different wavelengths, six LEDs of each wavelength are on one module. Modules can be connected to expand the light unit. Table II gives an overview over the chosen LEDs and the individual wavelength. The light unit is capable of controlling the intensity of each wavelength type individually to control the illumination spectrum, and globally to control the overall intensity. The light unit is also capable of controlling “on – off” periods such as a flashing rhythm to induce the FLE, with periods around one second, and a day-night cycle with periods of 24 h.

At maximum intensity (all LEDs at 100%) of the illumination unit at 10 cm is  $1023 \mu\text{mol/s m}^2$ , measured with a Kipp & Zonen Par sensor PQS1. Below  $200 \mu\text{mol/s m}^2$  at 10 cm distance, some LEDs do not reach the required forward

current anymore. Therefore an operation at lower intensities must be achieved by using dimming screens of increasing the distance to the reactor surface.

Fig. 10 shows different illumination spectra, normalized on 660 nm compared to the absorption spectrum of *C. vulgaris*. The spectra were produced by the illumination unit and measured with a “Vernier SpectroVis Plus”

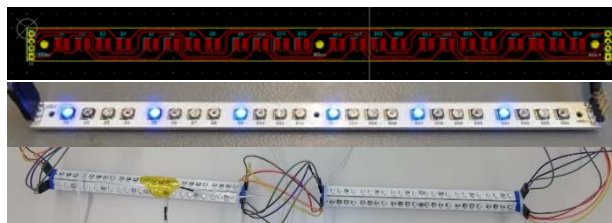


Fig. 9 Modular light unit with eight different wavelength LEDs

TABLE II  
CHOSEN LEDs FOR ILLUMINATION UNIT

LED	Wavelength [nm]
LV CQBP OSLO® Signal	505
OCI-440 680p	680
OCU-440 UE425	425
LCY CLBP OSLO® Signal	600
LUXEON 3535L Red-Orange	620
LUXEON 3535L Royal Blue	455
GH CSSRM2.24 OSLO®square	660
LUXEON 3535L Blue	480

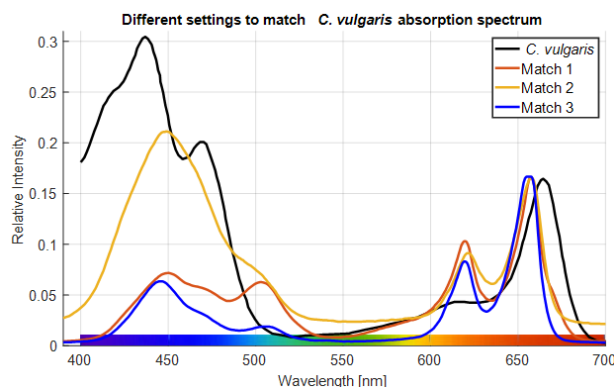
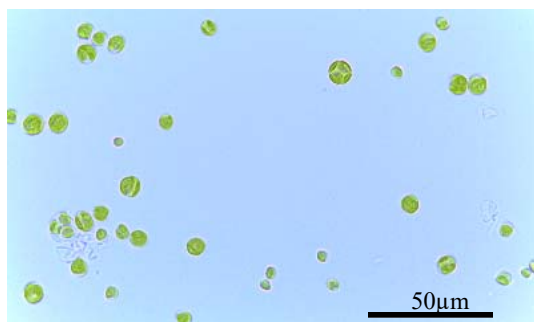


Fig. 10 Spectra of different settings

## V. MICROALGAE AND MEDIUM OF CULTIVATION

The type *Chlorella vulgaris* strain SAG 211-12 from the Department of Experimental Phycology and Culture Collection of Algae was chosen as microalgae for the cultivation due to its suitability for the named requirements [24]. Fig. 11 shows a microscopic picture of *C. vulgaris*. In order to validate the capability of the chosen microalgae to grow and absorb nitrogen from agricultural waste water with the chosen reactor setup, a tubular one-liter test reactor with adaptable light unit was built and a SGW was defined.

Fig. 11 Microscopic picture of *C. vulgaris*

## A. SGW

TABLE III

EVALUATION OF GW IONS OF LARGE SCALE STUDY COMPARED TO SGW

ingredient		Measured [mg/l]		Ingredient SGW [mg/l]
		median	main range	
chloride	Cl <sup>-</sup>	52	11-420	76.02
sulphate	SO <sub>4</sub> <sup>2-</sup>	197	30-550	197
sodium	Na	22	7 - 80	57.93
potassium	K	4.5	1-11	5.24
calcium	Ca	124	30-230	107.8
magnesium	Mg	21	6-50	15.3
nitrate	NO <sub>3</sub> <sup>-</sup>	140	100-367	146
ammonium	NH <sub>4</sub> <sup>+</sup>	1.2	0.5-13	2.73
nitrite	NO <sub>2</sub> <sup>-</sup>	-	0.005-0.05	-
phosphate	PO <sub>4</sub>	12	1.3-19.9	12.82
iron	Fe	0.5	0.005-5	0.56
manganese	Mn	0.09	0.1-0.6	0.43
aluminum	Al	1	2-14	5.06

To guarantee the reproducibility of experiments, a SGW needs to be defined. The GW constituents differ, depending on the nature of the soil and the use of the surface [25]. The selected composition is based on the report of the large-scale study on the condition of GW in Sachsen-Anhalt, as well as legal requirements of Germany for limit values [26], [27]. The study documented and evaluated GW constituents at 1244 measuring points between 2001 and 2010. For the composition of the SGW, salts, nutrients and trace substances were considered. Dissolved gases, organic substances, GW fauna and drug residues were not taken into account due to the reproducibility of the SGW. Heavy metals were also ignored, as their presence in GW represents a different type of environmental pollution, which is not dealt with by this project. The salts for the composition of the SGW were selected in such a way that the respective total concentrations of the individual ingredients are reproduced representatively, which means close to the median value and always within the main measuring range (defined as: 90% of the measurement results of the study lie within this range). For the nutrients nitrate, ammonium, nitrite and phosphorus, measured values from polluted agricultural land were used as a basis. The polluted areas were defined as the 10% agricultural used areas with the highest values of nitrate. Nitrite is a natural intermediate product in the microbial oxidation of ammonium to nitrate. Therefore, it was not considered as ingredient. Table

III gives an overview over the relevant components, the median and the range that was measured in the study and the amount that is present in the defined SGW. The nutrients that are relevant for pollution are based on polluted areas and are shaded in grey in the table. Table IV presents the selected salts and quantities per liter.

TABLE IV  
INGREDIENTS OF SALTS IN SGW

Salt	Solubility [g/l]	Content in SGW [mg/l]	Cation [mg/l]	Anion [mg/l]
NaCl	358	10	3.93	6.07
NaNO <sub>3</sub>	874	200	54.00	146.00
(NH <sub>4</sub> ) <sub>2</sub> SO <sub>4</sub>	754	10	2.73	7.27
KCl	347	10	5.24	4.76
CaSO <sub>4</sub>	2.4	340	100.10	239.90
FePO <sub>4</sub>	0.2	1.5	0.56	0.94
MnCl <sub>2</sub>	723	1	0.47	0.56
AlCl <sub>3</sub>	450	25	5.06	19.94
MgCl <sub>2</sub>	1670	60	15.30	44.70
CaHPO <sub>4</sub>	0.1	17	4.99	11.87
Ca(OH) <sub>2</sub>	1.7	5	2.71	2.26

## B. Experiment Setup

Fig. 12 shows two one-liter test reactors with adaptable illumination unit that were used to run the experiments. The described experiments are listed in Table V with the number they are referred to in this paper.

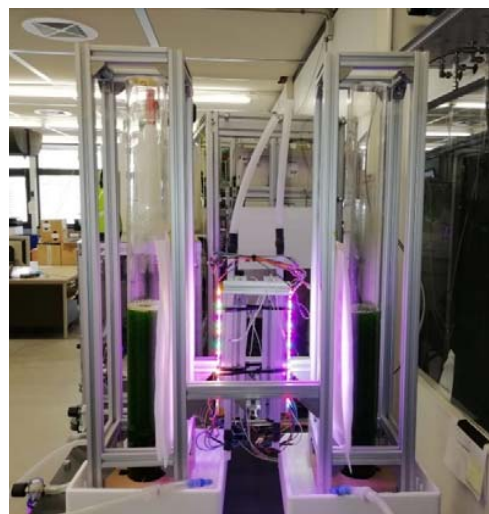


Fig. 12 Setup of two one-liter test reactor with adaptable light unit

TABLE V  
CONDUCTED EXPERIMENTS

Experiment Nr.	Goal
1	Demonstrate functionality of reactor setup
2	Demonstrate functionality and Nitrate uptake with SGW
3	Evaluate energetic efficiency of illumination strategy

## VI. CONDUCTED EXPERIMENTS

A first experiment was conducted to demonstrate the capability of the selected microalgae to grow in the chosen reactor type with the developed illumination unit. In order to



be able to compare the growth rates to other reactor types from literature, a cultivation in Dilluted Seawater Nitrogen medium DSN was conducted. This medium was introduced by Pohl [28] and is a standard cultivation medium used with *C. vulgaris*. The illumination was done with  $680 \mu\text{mol/s m}^2$  and illuminated from both sides of the reactor. The measured illumination spectrum is shown as “match 2” in Fig. 10. A flashing rhythm of 0.2 seconds of light and 0.8 seconds of darkness was set. This rhythm was kept over the whole time - no Day-Night cycle was implemented. The reactor was

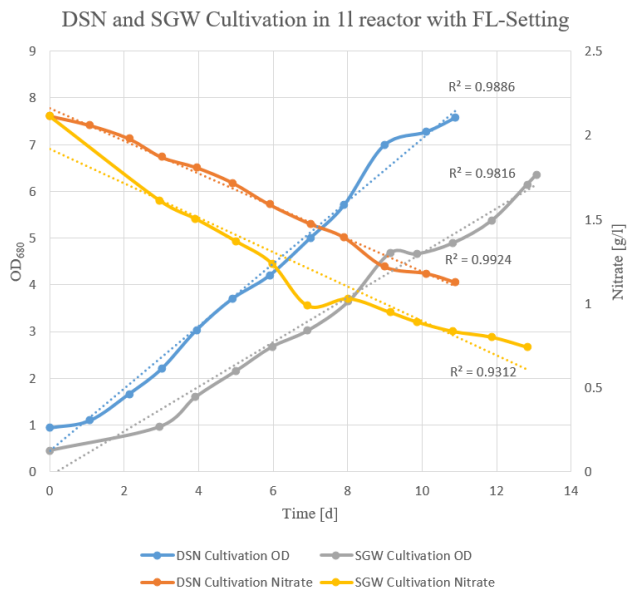


Fig. 13 OD and Nitrate concentration of Exp. 1 & 2

After successful cultivation over 11 days, a similar experiment was conducted with SGW. For this experiment,

however, the illumination had to be reduced due to the lower starting optical density (OD). The measured illumination density at the reactor surface was  $245 \mu\text{mol/s m}^2$  and the measured illumination spectrum is shown as “match 3” in Fig. 10. The same flashing rhythm as in exp. 1 was kept. Fig. 13 shows the measured absorption at 680 nm and the nitrate concentration of both experiments. The growth rates cannot be compared directly due to the different starting point and illumination scenario, but the experiments proved that the reactor setup is functional and nitrate can be absorbed from SGW through microalgae cultivation in this reactor type. For the cultivation in SGW at low light levels, the growth rate per  $\mu\text{mol/s m}^2$  is higher than for cultivation at high intensities in DSN, this may be caused by the effect of the room illumination.

Next, the effect of the FLE on the energetic efficiency of growth rate and nitrate uptake rates was subject of investigation. To compare the growth rate related to the intensity of illumination, two cultivation runs were made. Each run was conducted in two reactors, as shown in Fig. 12. For the first run, the illumination unit was set to constant illumination and to the spectrum “match 1” as shown in Fig. 10. The illumination intensity was reduced to  $45 \mu\text{mol/s m}^2$  at the front of the reactor with silicone films. For the second run, the illumination frequency was switched to 0.3 s of light period and 0.7 s of dark period. The spectrum and the maximal intensity at the reactor surface were kept constant. Both experiments were conducted with DSN medium and started with a  $\text{NO}_3^-$  concentration of 300 mg/l and a  $\text{PO}_4$  of 200 mg/l. The fumigation was 0.5 l/min with 10%  $\text{CO}_2$ .

Figs. 14 and 15 show the measured data of both runs. The shown equations are linear fits to the growth rates. The measured OD at 680 nm can be correlated to the biomass dry weight with a linear relation with the factor of 0.23 [29].

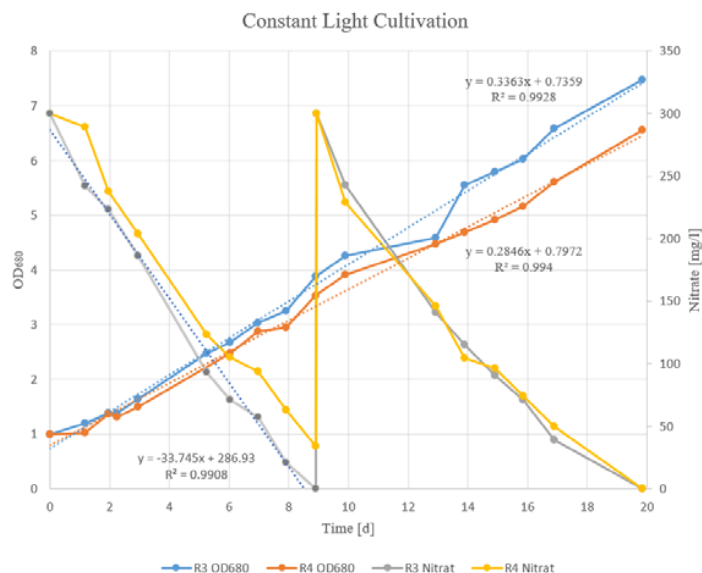


Fig. 14 OD and Nitrate concentration of Exp. 3 Run 1

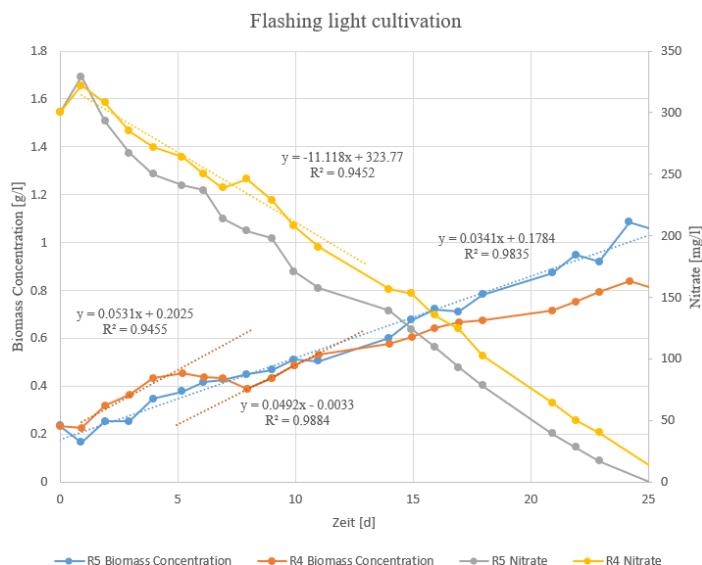


Fig. 15 OD and Nitrate concentration of Exp. 3 Run 2

Table VI summarizes the results of the experiment. The illumination intensity is averaged for the FLE setting and the growth rate related to the intensity of illumination is calculated from this value. The “energetic efficiency” of the system, related to biomass production more than doubled, and the “energetic efficiency” of the nitrate uptake rate was almost doubled.

TABLE VI  
CONDUCTED EXPERIMENTS

Illumination [ $\mu\text{mol/s m}^2$ ]	Growth rate [g/l·d]	$\text{NO}_3$ rate [mg/l·d]	Growth rate rel. to light energy [mg/l·d $\mu\text{mol/s m}^2$ ]	$\text{NO}_3$ rate rel.to light energy [mg/l·d $\mu\text{mol/s m}^2$ ]
45	0.0773	33.745	1.72	0.75
13.5	0.0538	25.833	3.985	1.29

## VII. DISCUSSION CONCLUSION AND OUTLOOK

The conducted experiments proof that the chosen setup is capable of meeting the requirements. The experiments indicate that, with the developed illumination unit a significant reduction of the energy consumption can be achieved. For the illumination energy, only the photons at the reactor surface were taken into account. Losses through the illumination unit, caused by the control unit were not taken into account. In further investigations, the influence of the illumination spectrum, on the biological component of the system will be investigated. Furthermore, the energetic optimization of the physical components of the system will be considered.

## ACKNOWLEDGMENT

The implementation of this project was made possible by a grant from DLR Space Management. Project number 50RP1925. Parts of the work were financed by the support of the Friedrich und Elisabeth BOYSEN - Stiftung [BOY-139].

## REFERENCES

- [1] F. Wisotzky, N. Cremer, S. Lenk, Angewandte Grundwasserchemie, Hydrogeologie und hydrogeochemische Modellierung: Grundlagen, Anwendungen und Problemlösungen, 2. Auflage, Springer Spektrum, Berlin, 2018.
- [2] M. Kranert, Einführung in die Abfallwirtschaft, Morgan Kaufmann, [Place of publication not identified], 2015.
- [3] U. Prüße, K.-D. Vorlop, Entfernung von Nitrat aus Trinkwasser, CHEMKON 3 (1996) 62–67.
- [4] W. Römer, Vergleichende Untersuchungen zur Pflanzenverfügbarkeit von Phosphat aus verschiedenen P-Recycling-Produkten im Keimpflanzenversuch, J. Plant Nutr. Soil Sci. 169 (2006) 826–832.
- [5] C. Posten, Design principles of photo-bioreactors for cultivation of microalgae, Eng. Life Sci. 9 (2009) 165–177.
- [6] S. Abu-Ghosh, D. Fixler, Z. Dubinsky, D. Iluz, Flashing light in microalgae biotechnology, Bioresource technology 203 (2016) 357–363.
- [7] M. Calvin, Der Weg des Kohlenstoffs in der Photosynthese Nobel-Vortrag am 11. Dezember 1961, Angew. Chem. 74 (1962) 165–175.
- [8] J. Degen, A. Uebele, A. Retze, U. Schmid-Staiger, W. Trösch, A novel airlift photobioreactor with baffles for improved light utilization through the flashing light effect, Journal of Biotechnology 92 (2001) 89–94.
- [9] H. Helisch, J. Keppler, J. Bretschneider, S. Belz, S. Fasoulas, Preparatory ground-based experiments on cultivation of *Chlorella vulgaris* for the ISS experiment PBR@LSR, 2016.
- [10] H. Helisch, S. Belz, J. Keppler, G. Detrell, N. Henn, S. Fasoulas et al., Non-axenic microalgae cultivation in space – Challenges for the membrane  $\mu\text{PBR}$  of the ISS experiment PBR@LSR, Albuquerque, New Mexico, 2018.
- [11] M.F. Blair, B. Kokabian, V.G. Gude, Light and growth medium effect on *Chlorella vulgaris* biomass production, Journal of Environmental Chemical Engineering 2 (2014) 665–674.
- [12] R. Filali, S. Tebbani, D. Dumur, S. Diop, Estimation of *Chlorella vulgaris* growth rate in a continuous photobioreactor, Proceedings of the 18th World CongressThe International Federation of Automatic Control (2011) 6230–6235.
- [13] J. Martin, J. Keppler, G. Detrell, H. Helisch, R. Ewald, S. Fasoulas, Microalgae-based Photobioreactors for a Life Support System of a Lunar Base, Boston, USA, 2019.
- [14] Y.-K. Lee, Microalgal mass culture systems and methods: Their limitation and potential, Journal of Applied Phycology 13 (2001) 307–315.
- [15] F.G.A. Fernández, F.G. Camacho, J.A.S. Pérez, J.M.F. Sevilla, E.M. Grima, A model for light distribution and average solar irradiance inside outdoor tubular photobioreactors for the microalgal mass culture, Biotechnol. Bioeng. 55 (1997) 701–714.
- [16] H. Kindl, Biochemie der Pflanzen, Vierte, völlig neubearbeitete und

- aktualisierte Auflage, Springer Berlin Heidelberg, Berlin, Heidelberg, 1994.
- [17] C. Mildenerberger, Development of an illumination unit with an adaptive spectrum for microalgae cultivation: Masters Thesis supervised by J. Martin, Stuttgart, 2019.
  - [18] Z. Amini Khoeyi, J. Seyfabadi, Z. Ramezanzpour, Effect of light intensity and photoperiod on biomass and fatty acid composition of the microalgae, *Chlorella vulgaris*, *Aquacult Int* 20 (2012) 41–49.
  - [19] D.P. Maxwell, S. Falk, C.G. Trick, N. Huner, Growth at Low Temperature Mimics High-Light Acclimation in *Chlorella vulgaris*, *Plant physiology* 105 (1994) 535–543.
  - [20] H. Helisch, J. Keppler, G. Detrell, S. Belz, R. Ewald, S. Fasoulas et al., High density long-term cultivation of *Chlorella vulgaris* SAG 211-12 in a novel microgravity-capable membrane raceway photobioreactor for future bioregenerative life support in SPACE, *Life Sciences in Space Research* (2019).
  - [21] D.G. Kim, C. Lee, S.-M. Park, Y.-E. Choi, Manipulation of light wavelength at appropriate growth stage to enhance biomass productivity and fatty acid methyl ester yield using *Chlorella vulgaris*, *Bioresource technology* 159 (2014) 240–248.
  - [22] A.C. Ley, D.C. Mauzerall, Absolute absorption cross-sections for Photosystem II and the minimum quantum requirement for photosynthesis in *Chlorella vulgaris*, *Biochimica et Biophysica Acta (BBA) - Bioenergetics* 680 (1982) 95–106.
  - [23] R.J. Porra, W.A. Thompson, P.E. Kriedemann, Determination of accurate extinction coefficients and simultaneous equations for assaying chlorophylls a and b extracted with four different solvents: verification of the concentration of chlorophyll standards by atomic absorption spectroscopy, *Biochimica et Biophysica Acta (BBA) - Bioenergetics* 975 (1989) 384–394.
  - [24] J. Martin, G. Detrell, R. Ewald, S. Fasoulas, Scalable Microalgae-based Life Support System, Washington, USA, 2019.
  - [25] G. Mattheß, Die Beschaffenheit des Grundwassers, 3., überarb. Aufl., Borntraeger, Berlin, 2009.
  - [26] Bundesministerium für Umwelt, Naturschutz, Bau und Reaktorsicherheit, Nitratbericht 2016: Gemeinsamer Bericht der Bundesministerien für Umwelt, Naturschutz, Bau und Reaktorsicherheit sowie für Ernährung und Landwirtschaft, 2017.
  - [27] Gewässerkundlicher Landesdienst, Bericht zur Beschaffenheit des Grundwassers in Sachsen-Anhalt 2001 – 2010, 2012.
  - [28] P. Pohl, M.K. Ohlhase, S.K. Rautwurst, K. Laus-Kinnerk Baasch, An inexpensive inorganic medium for the mass cultivation of freshwater microalgae, *Phytochemistry* 26 (1987) 1657–1659.
  - [29] H. Helisch, J.-K. Chack, S. Fasoulas, F. Lapierre, A.G. Heyer, Close the gap – Potential of microalgal biomass for Closed ECLSS and future in-situ resource utilization in space, Boston, USA, 2019